Validation Flight Experiment for a Sounding Balloon Photovoltaic-based Attitude Determination System

Giuseppe Cataldi
Dept. of Civil and Industrial Eng.
Università di Pisa
Pisa, Italy
giuseppe.cataldi@dici.unipi.it

Matteo Gemignani
Dept. of Civil and Industrial Eng.
Università di Pisa
Pisa, Italy
matteo.gemignani@dici.unipi.it

Salvo Marcuccio
Dept. of Civil and Industrial Eng.
Università di Pisa
Pisa, Italy
salvo.marcuccio@unipi.it

***Abstract*— Sounding balloons have proven to be a very effective low-cost method to bring scientific and commercial payloads to the near-space environment. In the frame of our ongoing effort towards the development of a small stratospheric platform with autonomous flying capabilities, we have undertaken the design and manufacture of a flight experiment to verify the possibility to perform onboard attitude determination using the solar cell power output measurements to complement the inertial sensor. The system is based on six low-cost terrestrial solar cells placed on the sides of a box-shaped gondola, lifted to about 34 km altitude by a weather balloon. We describe the system architecture, the results of the first experimental flight and the post-landing attitude reconstruction.**

Keywords*— *sounding balloon, attitude determination, near-space platform, solar cell

I. Introduction

The use of sounding balloons is a cost-effective way to reach the near-space environment, that is the part of the stratosphere up to an altitude of around 40 km. At such altitude, most of the atmosphere is below the vehicle so that the environment is quite similar to LEO (Air Mass 0) in terms of solar spectrum and cosmic rays, while background pressure is in the range of a few to a few tens of mbar; also, a large portion of the terrain can be observed from a good vantage point. For these reasons and thanks to their low cost and ease of operation, sounding balloons are gaining increasing popularity among the scientific community as an experimental platform.

The main operational restriction to the use of sounding balloons for remote sensing and scientific observations is the duration of flight, normally limited to about 2 hours of permanence at stratospheric altitudes. Due to the decrease of atmospheric pressure with altitude, latex or neoprene balloons expand continuously during ascent under the internal overpressure. Eventually, structural failure occurs at a certain maximum altitude, bursting the balloon and terminating the ascending part of the flight. The payload, usually in the range of 1 to 4 kg, returns to the ground with a parachute. Fig. 1 shows the balloon immediately before launch.

Efforts are underway to extend the operational functionality of such platforms through the development of stabilization systems aiming at controlling the platform altitude [1] so to extend flight duration. In parallel, attitude control of the gondola is sought [2], so to allow for proper operation of remote sensing systems and of a variety of other possible payloads. In order to reach such goals, onboard power availability is a key issue. Presently, most sounding balloon payloads are battery-powered, with strong limitations to the total quantity of energy that can be brought onboard. To overcome such limitations, the use of a photovoltaic power generation system is the most convenient choice, considering also that the cost of the solar panel is offset by the possibility to re-use the system after platform recovery at the end of the mission.

Fig. 1 Balloon at launch

II. Background and Motivations

Balloon research at University of Pisa is underway since several years [3, 4]. In the frame of the development of an advanced sounding balloon platform for scientific applications, our group has designed a photovoltaic power system based on flexible solar cells. The panel is body-mounted on the payload gondola and consists of a number of independent sections. A single solar cell's voltage can be interpreted as a measure of the incoming solar flux power, which essentially is a function of the payload orientation with respect to the Sun. Therefore, by knowing the relative position of the Sun and the platform at a given instant in time, the spatial arrangement of the onboard solar cells and the power generated by a certain number of them at different locations

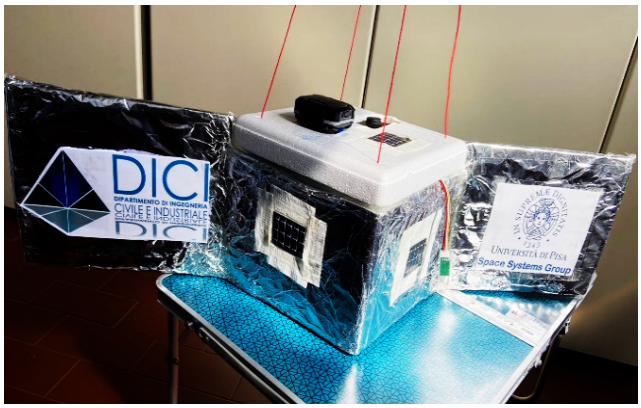

Fig. 2 Payload box assembled

around the gondola, it is possible in principle to reconstruct the orientation of the gondola with respect to a fixed reference system.

Nowadays, attitude determination of balloon gondolas is normally carried out by means of a miniaturized Inertial Measurement Unit (IMU). Measurements based on solar cell data are however a desirable complement to inertial readings, as they provide an absolute reference to perform sensor data fusion for in-flight correction of long term drift of the inertial sensors. In most MEMS-based IMUs, pitch and roll measurements are very accurate as they combine the information from both an accelerometer and a gyroscope. Yaw angle measurement, on the contrary, is obtained through a magnetometer; as a consequence, it is much less accurate and reliable. Therefore, provided that good knowledge of the Sun's elevation in the sky at the balloon's position is available, it is possible to determine with great accuracy the yaw angle by means of the solar cell measurement, thus making the balloon platform capable to operate independently. Such autonomous operation capability is highly desirable, whereas the requirement to maintain continuous communication with a ground station would make the system much less viable and attractive for applications.

In the past, various methods have been proposed for the exploitation of data from solar panels for attitude determination of spacecraft. [5] and [6] suggest the joint use of solar panel readings to improve the convergence of the Kalman filter applied to the magnetometer output. [7] analyses different satellite solar panel configurations acting as attitude sensors through the measurement of the short-circuit current and concludes that such system is suitable for low-cost space applications. Also, [8] considers the importance of solar panel current measurements to reconstruct the attitude of a generic satellite during the failure of an onboard wheel. [9] attempts to determine the satellite attitude through trigonometrical considerations based on solar panel's current with the knowledge of Sun position. In the model it is assumed that the incoming radiation is only direct light from the Sun. However, it is pointed out that, by neglecting the Earth albedo effect, large offsets might be introduced into the Sun position computation. For this reason it can be considered to use sampling techniques on a spherical region ([10], [11] and [12]) based on measurements from different solar cells located on various areas in order to determine the radiation distribution arriving on the satellite.

In this paper, we present the design and implementation of a preliminary version of an attitude determination system based on solar cells for the payload gondola of a sounding balloon and the results of the first experimental flight.

III. Experiment Description

The experimental system is hosted in a 22 x 22 x 19 cm aluminium-covered polystyrene box. Two fixed aerodynamic surfaces are attached external to the box (Fig. 2), to increase the front section and dampen yaw oscillations during ascent.

The architecture of the system is shown schematically in Fig. 3. Flexible solar cells are installed on each of the six sides of the box in order to obtain measurements of the incoming power fluxes from every direction. Each solar cell discharges the produced power on a 220 Ω resistor, while the generated voltage is measured through the analog input ports of the Arduino Uno R3 controller. Data from the controller and from the onboard Inertial Measurement Unit (IMU) are transferred to and stored by a Raspberry Pi 3 through USB serial communication for the former and I2C serial communication for the latter. The payload also includes a 3-axis gyroscope

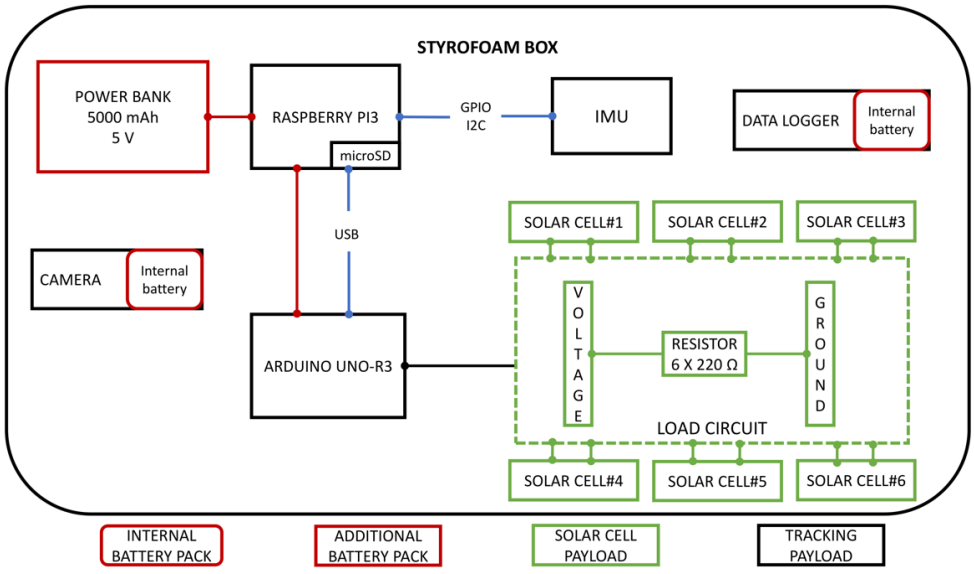

Fig. 3 Block diagram of the payload architecture

used to collect data about box angular speeds, useful for sensor fusion post-processing. In addition, two video cameras capable of 1080p, 30 fps recording have been positioned on the upper face and on one of the lateral sides, respectively, in order to have visual control of the flight attitude. A commercial data logger collects atmospheric data and acquires the balloon position during the flight via a GNSS receiver. Finally, an additional GNSS tracker accessible through a satellite link is included to allow post-landing recovery of the assembly. The total mass of the box including all internal components is about 1.5 kg. Launch is performed using a commercial 1600 g rubber-latex sounding balloon, equipped with a parachute. The balloon is sized so to lift the payload box up to a nominal altitude of about 30 km.

When the flight is over and the box has been recovered at the landing site, data collected from solar cell measurements are processed to reconstruct the attitude history. In order to demonstrate the validity of the solar cell-based attitude determination model, the results of the analysis are to be cross-checked with the IMU's data.

IV. Photovoltaic Sensor Model

Assuming that the Sun is the only source of radiation, the voltage generated by a solar cell V is expressed as a function of the radiation angle of incidence θ by the equation:

$$V(\theta) = V_0 \cos\theta \tag{1}$$

where $V_0 = V\ (\theta = 90°)$. Under ideal conditions, assuming similar properties for each cell, it is therefore possible to reconstruct the direction of the Sun in the body reference system $\hat{\boldsymbol{r}}^B$ through the voltages measured by three cells orthogonally arranged to the main axes of the payload. However, in real cases the measurement is affected by noise due to the diffuse radiation in the operating environment. For this reason it is necessary to use six cells, two for each body's principal axis, so that the intensity of the radiation can be detected on the sides not in view of the Sun, in order to determine which faces are subject to direct radiation by comparison. In [13] and [14] each component of the Sun direction is determined simply by subtracting the measurements obtained from the cell in the negative directions of the reference system V_i^- from that in the positive ones V_i^+:

$$r_i^B = \Delta V_i = V_i^+ - V_i^- \tag{2}$$

This approach is certainly the most direct one, but in case of strong diffuse radiation the resulting value of the components is underestimated. The method proposed here also uses the difference between the voltages, but the i-th component of the Solar direction is determined taking into account the entity of this value according to the following law:

$$r_i^B = f(V_i^+, V_i^-) = \frac{V_i^+ + V_i^-}{1+\exp(-\Delta V_i)} - V_i^- \tag{3}$$

Eq. (3) is an example of *logistic function*. The choice is motivated by the fact that for high absolute values of ΔV_i, the module and the sign of the component are determined only by the voltage of the most illuminated cell regardless of the amount of radiation present in the environment. On the contrary, when $\Delta V_i \approx 0$, the component linearly varies between the two values V_i^+ and V_i^-, similarly to Eq. (2).

In this way, after a simple vector normalization, the resulting Sun direction in the body-reference frame takes the form $\hat{\boldsymbol{r}}^B = \left[r_x^B, r_y^B, r_z^B\right]$. At this point, knowing the Sun position in the global reference system $\hat{\boldsymbol{r}}^G = \left[r_x^G, r_y^G, r_z^G\right]$, it is possible to estimate the heading angle of the payload. To do this we consider the projections of both vectors in the *x*-*y* planes of the respective reference systems and we determine the counter-clockwise angles formed with an arbitrary direction. In our case, the *x* axis was chosen, as it complies with the gyroscope measurement reference system. Therefore, angles A_G and A_B are obtained from:

$$A_G = atan2\left(r_y^G, r_x^G\right)$$

$$A_B = atan2\left(r_y^B, r_x^B\right)$$

The heading angle A_H is obtained through their difference:

$$A_H = mod(A_B - A_G, 2\pi) \in [0, 2\pi) \tag{4}$$

where $mod(\,)$ is the modulus operator. Equation (4) becomes inaccurate for high values of the tilt angles with respect to the local horizontal plane. This case does not occur during the ascending phase of our experiment due to the balloon inertia that prevents tilt rotations.

V. Sensor Fusion Model

The sensor fusion between solar cells and gyroscope measurements is performed by solving a Least Squares Estimation (LQE) or Kalman filtering problem. The heading angle A_H is estimated using the angular rate of the gyroscope $\dot{A}_H$ considering also a bias component $\dot{A}_d$ that represents the drift disturbance. The system's Linear Time-Invariant (LTI) discrete model has the form:

$$\boldsymbol{x}_{k+1} = \boldsymbol{A}\boldsymbol{x}_k + \boldsymbol{B}u_k + \boldsymbol{G}\boldsymbol{w}_k \tag{5}$$

$$y_k = \boldsymbol{C}\boldsymbol{x}_k + v_k$$

with $\boldsymbol{A} = \begin{bmatrix} 1 & \Delta t \\ 0 & 1 \end{bmatrix}$, $\boldsymbol{B} = \begin{bmatrix} \Delta t \\ 1 \end{bmatrix}$, $\boldsymbol{G} = \begin{bmatrix} 1 & 0 \\ 0 & 1 \end{bmatrix}$ and $\boldsymbol{C} = [1 \quad 0]$. The terms in Eq. (5) are listed in Table 1, while a schematic of the system's model is shown in Fig. 4.

TABLE I. List of terms contained in the system LTI model

System Variable	Description
$\boldsymbol{x}_k^T = \left[A_H, \dot{A}_d\right]_k$	k-th vector state
$u_k = \left(\dot{A}_H\right)_k$	k-th input vector
$\boldsymbol{w}_k^T = [w_{A_H}, w_{\dot{A}_d}] \sim N(\boldsymbol{0}, \boldsymbol{Q}_w)$	zero-mean Gaussian process noise vector
$y_k = (A_H)_{out}$	k-th system output vector
$v_k = v_{A_H} \sim N(0, R_v)$	zero-mean Gaussian measurement noise

The state component $\dot{A}_d$ is defined as a *pure input disturbance*, because it affects only the estimation model and not the measurement one. The matrix $\boldsymbol{G}$, instead, has been chosen equal to identity because the uncertainties due to process noises are unknown.

Let's assume that $\hat{\boldsymbol{x}}_k$ is the k-th *estimated vector state*, $\boldsymbol{P}_k$ is the k-th *estimate error covariance matrix*; then we formulate a state estimator in the form:

$$\hat{\boldsymbol{x}}_{k+1,k} = \boldsymbol{A}\hat{\boldsymbol{x}}_{k,k} + \boldsymbol{B}u_k$$

$$\boldsymbol{P}_{k+1,k} = \boldsymbol{A}\boldsymbol{P}_{k,k}\boldsymbol{A}^T + \boldsymbol{Q}_w$$

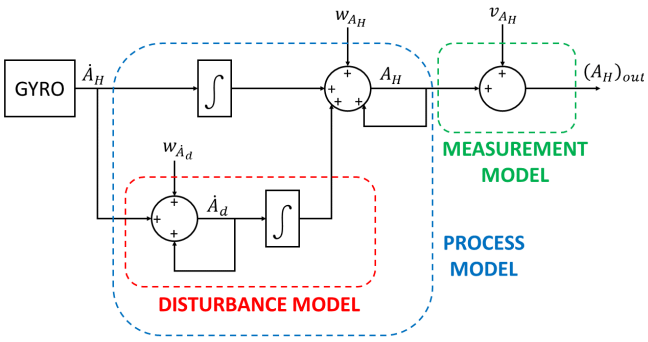

Fig. 4 Schematic of the system

$$\boldsymbol{K}_{k+1} = \boldsymbol{P}_{k+1,k}\boldsymbol{C}^T\left(\boldsymbol{C}\boldsymbol{P}_{k+1,k}\boldsymbol{C}^T + R_v\right)^{-1} \quad (6)$$

$$\hat{\boldsymbol{x}}_{k+1,k+1} = \hat{\boldsymbol{x}}_{k+1,k} + \boldsymbol{K}_{k+1}z_k$$

$$\boldsymbol{P}_{k+1,k+1} = (\boldsymbol{I} - \boldsymbol{K}_{k+1}\boldsymbol{C})\boldsymbol{P}_{k+1,k}$$

where $z_k = y_k - \boldsymbol{C}\hat{\boldsymbol{x}}_{k,k-1}$ is the *innovation* and $\boldsymbol{K}$ is the *Kalman gain*. The Kalman gain is an index of the relationship between uncertainty due to the estimation and that due to the measurement. $\boldsymbol{K}$ is the optimal value of gain that minimizes the measurement error from the real value.

VI. Estimation of the Optimal Gain

The characteristics of instruments noise are not known and this is a serious limit on the correct implementation of the filter. The method most recommended in the literature ([15] - [19]) for the determination of noise is the *Autocovariance Least Squares* (ALS) algorithm. Given an estimation and a measurement model, this method allows to estimate the correct values of the covariance matrices $\boldsymbol{Q}_w$ and R_v based on generic measurements in operating conditions. It can be demonstrated that the resolution of the ALS problem leads to a semi-definitive constrained optimization problem. Several versions will be introduced later in the paragraph. For a well-explained and developed treatment of the ALS analytical formulation see the cited works.

The autocovariance is defined as the covariance of the process itself calculated by pairs of time points. In particular, given a set of N_d collected data, and a generic (not optimal) gain $\boldsymbol{L}$, the LQE problem is simulated according to:

$$\hat{\boldsymbol{x}}_{k+1,k} = \boldsymbol{A}\hat{\boldsymbol{x}}_{k,k} + \boldsymbol{B}u_k$$

$$\hat{\boldsymbol{x}}_{k+1,k+1} = \hat{\boldsymbol{x}}_{k+1,k} + \boldsymbol{L}Y_k \quad (7)$$

where $Y_k = y_k - \boldsymbol{C}\hat{\boldsymbol{x}}_{k,k-1}$ stands for the *L-innovation*. At this point, the autocovariance between different times of Y_k distribution is determined. A user-defined parameter $N \ll N_d$ is introduced, which corresponds to the maximum time lag used for the autocovariance calculation. Hence, the L-innovation autocovariance with time lag j is estimated by the relationship:

$$\hat{C}_j = \frac{1}{N_d - j}\sum_{i=1}^{N_d-j} Y_i\, Y_{i+j} \quad (8)$$

for $j = 0{:}\,N-1$. The results are collected in the L-innovation autocovariance matrix (ACM) by the form:

$$\hat{\boldsymbol{R}} = \begin{bmatrix} \hat{C}_0 & \cdots & \hat{C}_{N-1} \\ \vdots & \ddots & \vdots \\ \hat{C}_{N-1} & \cdots & \hat{C}_0 \end{bmatrix} \quad (9)$$

Since an initial generic $\boldsymbol{L}$ gain has been chosen, the ACM has nonzero off-diagonal terms, while for optimal gain values the matrix tends to be diagonal. According to [18], Eq. 9 leads to a semi-definite constrained least squares problem formulation:

$$\min_{\boldsymbol{x}} \frac{1}{2}\left(\tilde{\boldsymbol{A}}\boldsymbol{x} - \tilde{\boldsymbol{b}}\right)^T\left(\tilde{\boldsymbol{A}}\boldsymbol{x} - \tilde{\boldsymbol{b}}\right) \quad (10)$$

$$\text{with } \begin{cases} \boldsymbol{Q}_w \geq 0 \\ R_v \geq 0 \end{cases}$$

where $\boldsymbol{x}^T = [vec(\boldsymbol{Q}_w), R_v]$ and $vec()$ is the vectorization operator. However, since a matrix $\boldsymbol{G} = \boldsymbol{I}$ was chosen, the uniqueness of the solution is not ensured. In this case, as [17] suggests, it is only possible to determine the optimal value of the gain $\boldsymbol{L}$, solving the problem:

$$\min_{\boldsymbol{x}_G} \frac{1}{2}\left(\boldsymbol{A}_1\boldsymbol{x}_G - \hat{\boldsymbol{R}}_1\right)^T\left(\boldsymbol{A}_1\boldsymbol{x}_G - \hat{\boldsymbol{R}}_1\right) \quad (11)$$

$$\boldsymbol{L} = \boldsymbol{P}\boldsymbol{C}^T(\boldsymbol{C}\boldsymbol{P}\boldsymbol{C}^T + R_v)^{-1}$$

where $\boldsymbol{x}_G^T = [\boldsymbol{P}\boldsymbol{C}^T, R_v]$. Given the strong non-linearity of this problem, it can be solved iteratively. Starting from an initial guess of $\boldsymbol{L}$, the estimation model is simulated in accordance with Eqs. 7, then the L-innovation autocovariances are calculated and the minimum solution of (11) is determined. Substituting the minimum $\boldsymbol{x}_G$ in the latter expression of Eq. 11 we obtain a new value of the gain with which the procedure is repeated until convergence is achieved.

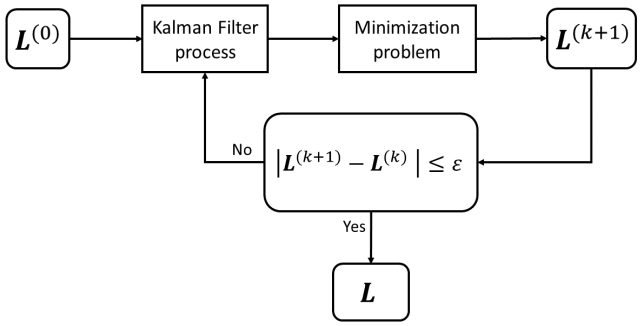

Fig. 5 Block diagram of the algorithm.

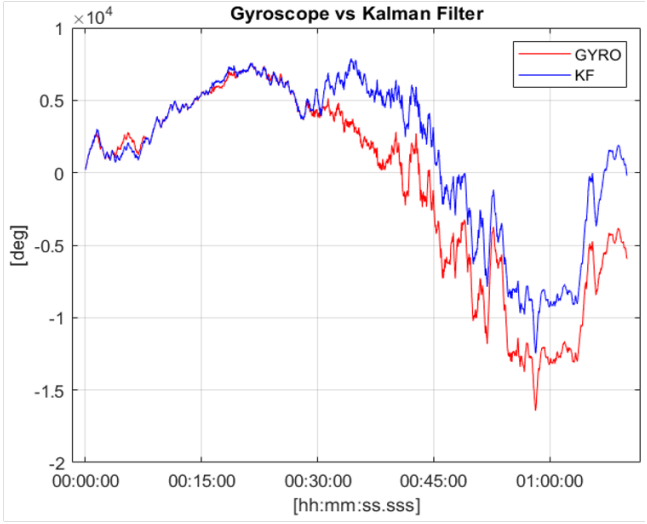

Fig. 6 Yaw angle form raw gyro data vs. filtered estimate.

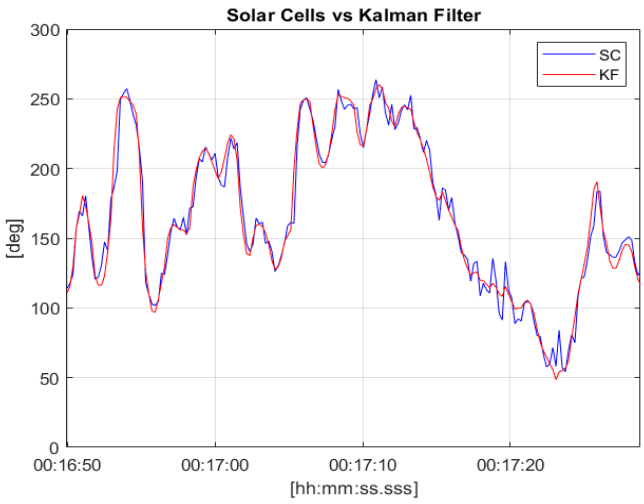

Fig. 7 Solar cell data vs. Kalman filter output

VII. Results

Launch of the balloon took place from Lajatico (Pisa, Italy) on March 7 at 10:50 in cloudy weather. The balloon reached an altitude of 34583 m before exploding. The payload landed on parachute about 20 km from the launch site. The total flight duration was approximately 2 hours and 30 minutes.

Following the experiment, an attempt was made to formulate a correct implementation of a sensing fusion algorithm between the gyroscope and solar cells through the data collected. The portion of the flight taken in consideration includes the portion of the ascent phase from immediately above the top of the clouds up to the balloon burst altitude. The minimization problem (Eq. 11) has been solved using the algorithm shown in Fig. 5, and then the optimal autocovariance matrix has been calculated. This matrix was used as an estimate of the covariance matrices employed in Kalman filtering.

Fig. 6 shows yaw angle the unfiltered output of the gyro vs. the output of the Kalman filter including contributions of the IMU's accelerometers and magnetometer. The horizontal axis shows time from the moment the balloon emerged above the cloud layer until burst, for about 70 min of total duration. Angular displacement on the vertical axis, given as a cumulative value from launch, shows values largely in excess of 360 deg corresponding to multiple turns of the gondola around the yaw axis. These are probably the combined result of the dynamics of the carrier balloon and of the gondola suspension lines own torsional dynamics.

The yaw angle as measured by the gyroscope and as resulting by Kalman-filtering the solar cell data over a representative period of about 40 s is shown in Fig. 7, demonstrating good agreement between the solar cell estimate and the filtered result.

VIII. Conclusions

The use of solar cells for attitude determination represents an innovation for the field of sounding balloons. Considering the stringent mass limits of these platforms we strongly believe that this sort of experiments, which are essentially based on extending the components function over their initial scope, represents the right path for the development of sounding balloon- borne platforms. Obviously the cells arrangement on the platform plays a key role in the trade-off between power generation and attitude determination, so the implementation of this method shall be adapted to future and more complex configurations.

Different techniques could be used in the future to improve the sensor fusion quality. Better knowledge of the noise characteristics of the sensors is needed; to this end, a possible strategy is to get a better in-flight evaluation of the low-cost solar cells used, by means of test flights dedicated to sensor performance characterization. A further possibility is to replicate stratospheric lighting conditions in a dark room and to correlate cell voltages to pyranometer measurements, so that it is possible to have more realistic indications about the behavior of the cells. As an alternative, different, more expensive but better characterized solar cells could be employed.

Acknowledgments

The authors wish to thank Mr. Giacomo Bertolucci, Ms. Alessia Gervasi, Mr. Alberto Manzini and Mr. Mattia Vinci for their valuable support during launch and payload recovery operations.

References

[1] Sushko A. et al., "Low-Cost, High Endurance, Altitude-Controlled Latex Balloon for Near-Space Research (ValBal)", IEEE, Big Sky, MT, 2017. doi: 10.1109/AERO.2017.7943912

[2] Nguyen Khoi Tran, Xiao He, David E. Zlotnik and James R. Forbes, "Attitude Sensing and Control of a Stratospheric Balloon Platform", AIAA 2013-1373, AIAA Balloon Systems (BAL) Conference, Daytona Beach, Florida, 2013. doi: 10.2514/6.2013-1373

[3] Gemignani, M., Marcuccio, S., "Flight Campaign Results and Prospects of High-Altitude Balloons for Low Cost Spacecraft Technology Testing", Proc. 25th AIDAA Conference, Rome, Italy, September 9-12, 2019, pp. 939-955. ISBN 978-88-943960-1-02

[4] Gemignani, M., Marcuccio, S., "Dynamic Characterization of a High-Altitude Balloon during a Flight Campaign for the Detection of ISM Radio Background in the Stratosphere". Aerospace. 2021; 8(1):21. https://doi.org/10.3390/aerospace8010021

[5] Svartveit K., "Attitude determination of the NCUBE Satellite", Master Thesis, Jun 20th 2003, Norwegian University of Science and Technology.

[6] Davydov A.A., "Determination of Parameters of Attitude Motion of a Small Communication Satellite Using the Data of Measurements of

Current of Solar Panels", Cosmic Research, 2011, vol. 49, no. 4, pp. 335-344. doi: 10.1134/S0010952511030051

[7] Nygren M., "Using Solar Panels as Sun Sensors on NTNU Test Satellite", Master Thesis, Dec 22nd 2002, Norwegian University of Science and Technology.

[8] Humphreys T. E., "Attitude Determination for Small Satellites Using Magnetometer and Solar Panel Data", Utah Space Grant Consortium, 2002, session 1.

[9] Rocha R., Rodrigues L., "Photovoltaic panels as attitude sensors for artificial satellites", IEEE Aerospace and Electronic Systems Magazine, Nov 2016, vol. 31, no. 11, pp. 14-23. doi: 10.1109/MAES.2016.150186

[10] Khalid Z., Kennedy R. A., McEwen J. D., "An Optimal-Dimensionality Sampling Scheme on the Sphere With Fast Spherical Harmonic Transforms", IEEE, Transactions on Signal Processing, 2014, vol. 62, no. 17, pp. 4597-4610. doi: 10.1109/TSP.2014.2337278

[11] Werner D. H., Allard R. J., "The simultaneous interpolation of antenna radiation patterns in both the spatial and frequency domains using model-based parameter estimation", IEEE, Transactions on Antennas and Propagation, 2000, vol. 48, no. 3, pp. 383-392. doi: 10.1109/8.841899

[12] Allard R. J., Werner D. H., "The model-based parameter estimation of antenna radiation patterns using windowed interpolation and spherical harmonics", IEEE, Transactions on Antennas and Propagation, 2003, vol. 51, no. 8, pp. 1891-1906. doi: 10.1109/TAP.2003.815419

[13] E. P. Babcock, "CubeSat Attitude Determination via Kalman Filtering of Magnetometer and Solar Cell Data", in 25th Annual AIAA/USU Conference on Small Satellites, Logan (Utah), 2011.

[14] S. Theil, P. Appel, A. Schleicher, "Low-Cost, Good Accuracy- Attitude Determination Using Magnetometer And Simple Sun Sensor", in 16th Annual AIAA/USU Conference on Small Satellites, Logan (Utah), 2004.

[15] B. M. Åkesson et al., "A Tool for Kalman Filter Tuning", Computer Aided Chemical Engineering, Elsevier, Vol. 24, 2007, pp. 859-864. doi: 10.1016/S1570-7946(07)80166-0.

[16] B. M. Åkesson et al., "A generalized autocovariance least-squares method for Kalman filter tuning", Journal of Process Control, Vol. 18, Issues 7–8, 2008, pp. 769-779, doi: 10.1016/j.jprocont.2007.11.003.

[17] B. J. Odelson et al., "The Autocovariance Least-Squares Method for Estimating Covariances: Application to Model-Based Control of Chemical Reactors", in IEEE Transactions on Control Systems Technology, vol. 14, no. 3, pp. 532-540, May 2006, doi: 10.1109/TCST.2005.860519.

[18] B. J. Odelson et al., "A new autocovariance least-squares method for estimating noise covariances", Automatica, Vol. 42, Issue 2, 2006, pp. 303-308, doi: 10.1016/j.automatica.2005.09.006.

[19] M. R. Rajamani, *Data-Based Techniques to Improve States-Estimation in Model Predictive Control,* University of Wisconsin-Madison, 2007.